A Section 508–conformant HTML version of this article is available at https://doi.org/10.1289/EHP6498.

Binding and Activity of Tetrabromobisphenol A Mono-Ether Structural Analogs to Thyroid Hormone Transport Proteins and Receptors

Xiao-Min Ren,[1,2] Linlin Yao,[1,2] Qiao Xue,[1,2] Jianbo Shi,[1,2,3,4] Qinghua Zhang,[1,2,3,4] Pu Wang,[4] Jianjie Fu,[1,2,3] Aiqian Zhang,[1,2,3] Guangbo Qu,[1,2,3,4] and Guibin Jiang[1,2,3]

[1]State Key Laboratory of Environmental Chemistry and Ecotoxicology, Research Center for Eco-Environmental Sciences, Chinese Academy of Sciences, Beijing, China
[2]University of Chinese Academy of Sciences (UCAS), Beijing, China
[3]Institute of Environment and Health, Hangzhou Institute for Advanced Study, UCAS, Hangzhou, China
[4]Institute of Environment and Health, Jianghan University, Wuhan, China

Background: Tetrabromobisphenol A (TBBPA) mono-ether structural analogs, identified as the by-products or transformation products of commercial TBBPA bis-ether derivatives, have been identified as emerging widespread pollutants. However, there is very little information regarding their toxicological effects.

Objective: We aimed to explore the potential thyroid hormone (TH) system–disrupting effect of TBBPA mono-ether structural analogs.

Methods: The binding potencies of chemicals toward human TH transport proteins [transthyretin (TTR) and thyroxine-binding globulin (TBG)] and receptors [TRα ligand-binding domain (LBD) and TRβ-LBD] were determined by fluorescence competitive binding assays. Molecular docking was used to simulate the binding modes of the chemicals with the proteins. The cellular TR-disrupting potencies of chemicals were assessed by a GH3 cell proliferation assay. The intracellular concentrations of the chemicals were measured by high-performance liquid chromatography and mass spectrometry.

Results: TBBPA mono-ether structural analogs bound to TTR with half maximal inhibitory concentrations ranging from 0.1 μM to 1.0 μM but did not bind to TBG. They also bound to both subtypes of TR-LBDs with 20% maximal inhibitory concentrations ranging from 4.0 μM to 50.0 μM. The docking results showed that the analogs fit into the ligand-binding pockets of TTR and TR-LBDs with binding modes similar to that of TBBPA. These compounds likely induced GH3 cell proliferation via TR [with the lowest effective concentrations (LOECs) ranging from 0.3 μM to 2.5 μM] and further enhanced TH-induced GH3 cell proliferation (with LOECs ranging from 0.3 μM to 1.2 μM). Compared with TBBPA, TBBPA-mono(2,3-dibromopropyl ether) showed a 4.18-fold higher GH3 cell proliferation effect and 105-fold higher cell membrane transportation ability.

Conclusion: This study provided a possible mechanism underlying the difference in TTR or TR binding by novel TBBPA structural analogs. These compounds might exert TH system–disrupting effects by disrupting TH transport in circulation and TR activity in TH-responsive cells. https://doi.org/10.1289/EHP6498

Introduction

Tetrabromobisphenol A (TBBPA) and its derivatives are applied as brominated flame retardants (BFRs) in the production of commercial products such as plastics, textiles, electronics and electrical equipment, light sockets, water pipes, and thermal insulation foam (Alaee et al. 2003; Liu et al. 2018). In addition to being used as an additive BFR, TBBPA (~ 18% of the production volume) is also used as a reactive BFR to synthesize TBBPA derivatives (Covaci et al. 2009; Liu et al. 2019; Qu et al. 2016). Commercial TBBPA bis-ether derivatives—such as TBBPA-bis(glycidyl ether) (TBBPA-BGE), TBBPA-bis(allyl ether) (TBBPA-BAE), and TBBPA-bis(2,3-dibromopropyl ether) (TBBPA-BDBPE)—are produced via modification of the hydroxyl groups (OH) on both sides of TBBPA with glycidyl ether, allyl ether, and 2,3-dibromopropyl ether groups, respectively (Figure 1) (European Commission 2006). Similar to TBBPA, TBBPA bis-ether derivatives have also been commonly used as additive or reactive BFRs to ultimately produce acrylonitrile butadiene styrene and high-impact polystyrene resins (Liu et al. 2018). Currently, TBBPA and its derivatives account for 60% of the total BFR market and have become the most widely applied BFRs in commercial products (Covaci et al. 2011).

In contrast to TBBPA bis-ether derivatives, TBBPA mono-ether structural analogs have only one OH group on the side of TBBPA replaced by a derivatized group. TBBPA mono-ether structural analogs—including TBBPA-mono(glycidyl ether) (TBBPA-MGE), TBBPA-mono(allyl ether) (TBBPA-MAE), and TBBPA-mono(2,3-dibromopropyl ether) (TBBPA-MDBPE)—are frequently detected. These chemicals could be synthesized as by-products during commercial TBBPA bis-ether derivative production (Qu et al. 2011). Some mono-ether structural analogs were detected in brominated epoxy resin samples at levels of 46–160 mg/kg (Liu et al. 2015). Furthermore, TBBPA mono-ether structural analogs could be generated from TBBPA bis-ether derivatives during transformation processes (Liu et al. 2018, 2019). Ether bond breakage was found to be an important transformation pathway for TBBPA bis-ether derivatives (Liu et al. 2017). TBBPA mono-ether structural analogs—including TBBPA-MGE, TBBPA-MAE, and TBBPA-MDBPE—could be transformed from commercial TBBPA bis-ether derivatives in the environment due to the breaking of ether bonds (Liu et al. 2016; Qu et al. 2013). Moreover, the substantially increased ratio of TBBPA-MAE/TBBPA-BAE (3.4:1) in the soil samples compared with the original ratio in the commercial products (9.2×10^{-3}:1) suggested that certain portions of TBBPA derivatives could transform to TBBPA mono-ether structural analogs in the environment (Liu et al. 2017). In addition, the biotransformation from TBBPA to some TBBPA mono-ether structural analogs has been reported in various studies (Chen et al. 2017; Gu et al. 2017), suggesting that TBBPA could also contribute to the occurrence of environmental TBBPA mono-ether structural analogs.

Address correspondence to Guangbo Qu, State Key Laboratory of Environmental Chemistry and Ecotoxicology, Research Center for Eco-Environmental Sciences, Chinese Academy of Sciences, 18 Shuangqing Rd., Beijing 100085, P. R. China. Telephone: 86-010-62849129. Email: gbqu@rcees.ac.cn

Supplemental Material is available online (https://doi.org/10.1289/EHP6498).

The authors declare they have no actual or potential competing financial interests.

Received 6 November 2019; Revised 23 September 2020; Accepted 30 September 2020; Published 23 October 2020.

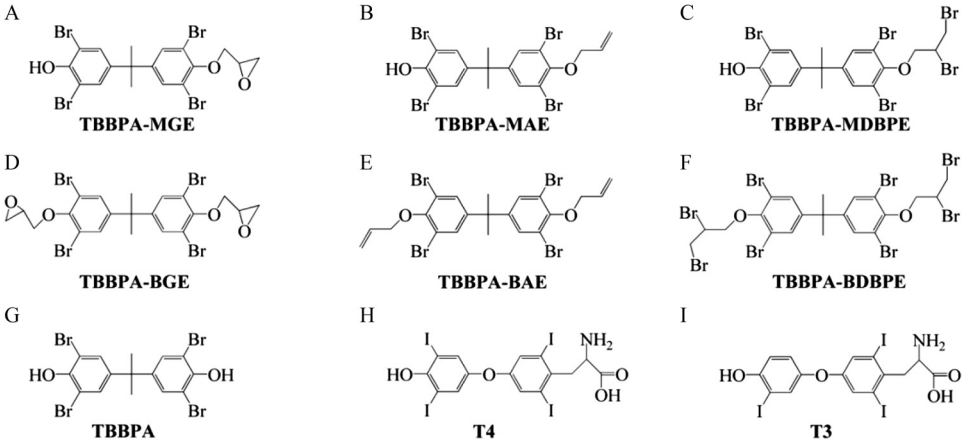

Figure 1. Chemical structures of the tested tetrabromobisphenol A (TBBPA) mono-ether structural analogs [(A) TBBPA-mono(glycidyl ether) (TBBPA-MGE), (B) TBBPA-mono(allyl ether) (TBBPA-MAE), and (C) TBBPA-mono(2,3-dibromopropyl ether) (TBBPA-MDBPE)], the tested TBBPA bis-ether derivatives [(D) TBBPA-bis(glycidyl ether) (TBBPA-BGE), (E) TBBPA-bis(allyl ether) (TBBPA-BAE), and (F) TBBPA-bis(2,3-dibromopropyl ether) (TBBPA-BDBPE)], (G) TBBPA, and the thyroid hormones [(H) thyroxine (T_4) and (I) triiodothyronine (T_3)].

Currently, because of their high production volume and wide application in consumer products, TBBPA and its derivatives are emerging as a group of ubiquitous pollutants that have been frequently detected in various environmental media, including river water, seepage water, sewage water, sediment (Nyholm et al. 2013; Qu et al. 2011), air samples (Liu et al. 2016), and wild animals (Letcher and Chu 2010; Liu et al. 2016). For example, TBBPA bis-ether derivatives and TBBPA mono-ether structural analogs were detected in the soil samples collected from sites around BFR production plants with levels ranging from below the method limit of detection (LOD) to 13 mg/g dry weight (Liu et al. 2017), and they were detected in some marine biological samples collected from the Chinese Bohai Sea with levels ranging from below the method LOD to 2.7 μg/g lipid weight (Liu et al. 2016). Some TBBPA bis-ether derivatives (such as TBBPA-BDBPE) and some TBBPA mono-ether structural analogs (such as TBBPA-MAE) were found at similar or higher levels than TBBPA in the samples collected from the same area (Liu et al. 2016, 2017). Evidence has shown that the contamination of TBBPA-BDBPE in herring gulls collected from Great Lake locations could be dated back to at least the early 2000s (Gauthier et al. 2019), suggesting that this chemical might have existed in the environment for a long time. The above studies suggest that humans might be exposed to these chemicals due to their release from commercial products containing TBBPA bis-ether derivatives added as BFRs or via exposure from environmental media contaminated by the pollution of BFR production plants. More importantly, TBBPA bis-ether derivatives and TBBPA mono-ether structural analogs have been identified in various types of seafood, including mollusks, shrimp, crab, and fish samples collected from coastal areas of the Chinese Bohai Sea (Liu et al. 2016). Consumption of contaminated seafood could lead to direct exposure to these chemicals through oral exposure and represents an important health concern.

Thyroid hormone (TH) plays an important role in maintaining a normal physiological state and is essential for central nervous system development, metabolism, and growth in mammals (Bernal 2005). Impaired TH function has been associated with many adverse health effects, such as deficient neurological development, reduced immune activity, obesity, and metabolic disorders (Yen 2001). When TH is produced and released from the thyroid gland into circulation, most of it binds to the TH transport proteins transthyretin (TTR) and thyroxine-binding globulin (TBG) (Brent 2012). In target tissues, TH exerts its biological actions by interacting with TH receptors (TRs) and regulating their activity in TH-responsive cells (Aagaard et al. 2011). To date, a large number of epidemiological studies have provided extensive data on the high prevalence and incidence of thyroid disease (Bjoro et al. 2000; Kwon et al. 2018). The prevalence of diagnosed thyroid dysfunction in the form of hypothyroidism was found to be 3.82% in Europe (Garmendia Madariaga et al. 2014). The incidence of thyroid cancer has tripled or more in many developed countries over the past 30 y (Roman et al. 2017). Iodine nutrition, aging, smoking status, and genetic susceptibility could be key determinants of thyroid disease risk (Taylor et al. 2018). Increasing evidence has shown that various environmental endocrine disruptors might also be an important driving factor (Boas et al. 2012; Hofmann et al. 2009; Jugan et al. 2010; Patrick 2009; Tang et al. 2020). Therefore, unveiling the molecular mechanisms responsible for pollutant exposure-associated thyroid disorders is critical to understanding the role of dominant environmental exposure factors in the increased incidence of thyroid disease.

One of the most concerning adverse effects of TBBPA is its endocrine-disrupting potency as a TH system–disrupting chemical (Wang et al. 2017; Yu et al. 2018; Zhang et al. 2014). Kim and Oh (2014) showed that TBBPA was weakly correlated with a disturbance in TH levels in the general population in Korea. Yang et al. (2016) demonstrated that THs presented a nonmonotonous dose–effect relationship in male Sprague-Dawley rats exposed to 0–1,000 mg/kg body weight (BW) per day and showed that the derived-reference dose was 0.6 mg/kg BW per day. By using zebrafish (*Danio rerio*) embryos, Zhu et al. (2018) demonstrated that TBBPA evoked TH system–disrupting effects by showing changes in the levels of THs and in the expression of some TH system-related genes after exposure to 200 μg/L TBBPA. TBBPA was reported to exert a TH system–disrupting effect via two possible mechanisms: *a*) through binding to TH transport proteins and disrupting TH homeostasis in blood (Meerts et al. 2000), or *b*) through binding to TRs and disturbing their activity and associated cellular functions (Chan and Chan 2012; Kitamura et al. 2002, 2005; Lévy-Bimbot 2012). In contrast to the extensive toxicity investigations already conducted on TBBPA, information concerning the toxicological effects of TBBPA bis-ether derivatives or TBBPA mono-ether structural analogs is limited. Understanding their structure-dependent activity on TH transport proteins or receptors is important to unveil the mechanisms underlying their effects on the TH system. Together with environmental exposure evaluation, investigation of the toxicity of TBBPA derivatives and

TBBPA structural analogs will help to clarify their potential health risks.

In the present study, we aimed to explore the characteristics of the disrupting potential of TBBPA derivatives and TBBPA structural analogs on the TH system. We chose three TBBPA derivatives (TBBPA-BGE, TBBPA-BAE, and TBBPA-BDBPE) and three TBBPA mono-ether structural analogs (TBBPA-MGE, TBBPA-MAE, and TBBPA-MDBPE) (Figure 1) that are most frequently detected in the environment. To study their potential TH transport-disrupting effects, we evaluated their binding potencies with two major human TH transport proteins (TTR and TBG). We also determined the binding potencies of these chemicals to two subtypes of human TR LBDs (TRα-LBD and TRβ-LBD). By using the GH3 cell proliferation assay, we evaluated their TR-disrupting potencies in cells. Molecular docking was used to simulate the binding modes of these chemicals with TH transport proteins and receptors. The cell membrane transportation ability between a TBBPA mono-ether structural analog and TBBPA was also compared by measuring their intracellular amounts in GH3 cells after exposure to investigate their effects and mechanisms.

Methods

Reagents

Human TRα-LBD (>85% purity) and TRβ-LBD (>85% purity) were prepared by Zhongding Biotechnology Co. Ltd. Human TTR (catalog no. 529577) and TBG (catalog no. 612075) were purchased from Calbiochem. Amiodarone (catalog no. A8423) was acquired from Sigma. 3,5,3′-Triiodothyronine (T_3) (catalog no. 30-AT53) was purchased from Fitzgerald Industries International, Inc. TBBPA (catalog no. 330396; 97%) was purchased from Alfa Aesar. TBBPA-BAE (catalog no. 17324750; 99%) and TBBPA-BDBPE (catalog no. 17324800; 99%) were purchased from Dr. Ehrenstorfer GmbH. TBBPA-BGE (catalog no. FRS-073N; 99%) was from AccuStandard. TBBPA-MAE, TBBPA-MDBPE, and TBBPA-MGE were synthesized in our previous work (Liu et al. 2015, 2016).

Fluorescence Competitive Binding Assays

Fluorescence polarization-based competitive binding assays were used to determine the binding potency of the chemicals to TH transport proteins and receptors. Two fluorescence probes, fluorescein-triiodothyronine (F-T_3) and fluorescein-thyroxine (F-T_4), were synthesized in our previous works (Ren and Guo 2012; Ren et al. 2013). F-T_3 and F-T_4 were prepared by reacting fluorescein isothiocyanate with T_3 or T_4, which resulted in derivatization of the amine groups of T_3 or T_4 with fluorescein. The competitive binding assays were carried out in a manner similar to a previous study (Qin et al. 2019). Briefly, 200 nM TTR and 50 nM F-T_4 were used in the TTR competitive binding assay, 100 nM TBG and 50 nM F-T_4 were used in the TBG competitive binding assay, and 200 nM TRα-LBD or 200 nM TRβ-LBD and 50 nM F-T_3 were used in the TR-LBD competitive binding assays. These assays were performed in potassium phosphate buffer [50 mM potassium phosphate, 150 mM potassium chloride (KCl), 0.5 mM ethylenediaminetetraacetic acid (EDTA), pH 7.5]. For the TTR and TBG competitive binding assays, five different concentrations of competitors were tested with the highest concentration of 50 μM and 10-fold dilutions between each of the other concentrations. For the TR-LBDs competitive binding assays, seven different concentrations of competitors were tested with the highest concentration of 50 μM and 2-fold dilutions between each of the other concentrations. The protein, probe, and different concentrations of competitor were mixed in a total volume of 100 μL and incubated for 5 min at room temperature (controlled at 25°C), and then the fluorescence polarization was measured. For the competitive binding assays, we prepared three replicate wells per experiment for each group in a 96-well plate. The dimethyl sulfoxide (DMSO) content was maintained below 1%. Fluorescence polarization was detected by a SpectraMax i3x multimode detection platform (Molecular Devices). The excitation and emission wavelengths were 490 nm and 520 nm, respectively. The fluorescence polarization value was plotted as a function of competitor concentration to obtain the competition curve. The values of half maximal inhibitory concentration (IC_{50}) or 20% maximal inhibitory concentration (IC_{20}), the concentration of a ligand required to displace 50% or 20%, respectively, of a probe from the protein) were obtained from the linear interpolation between two concentrations located at approximately the 50% or 20% inhibition level. The relative binding potency (RBP) was calculated by dividing the IC_{50} value of TBBPA (for TTR) or the IC_{20} value of TBBPA (for TRα-LBD and TRβ-LBD) by that of a competitor. The IC_{50}, IC_{20}, and RBP values (compared with TBBPA, which was set as 1) are listed in Table 1.

Molecular Docking Simulations

AutoDock Vina was used to simulate the interactions between the chemicals and TH transport proteins (or receptors). The crystal structures of TTR [Protein Data Bank identification number (PDB ID): 1ICT], TRα-LBD (PDB ID: 2H77), and TRβ-LBD (PDB ID: 1NAX) were obtained from The Research Collaboratory for Structural Bioinformatic (RCSB) Protein Data Bank (http://www.rcsb.org/pdb). The three-dimensional coordinates of the tested chemicals in PDB format were obtained through the PRODRG server (Schüttelkopf and van Aalten 2004). The water and ligands in the crystallized proteins were removed first. The grid center was chosen as the middle point of the co-crystallized ligand. The grid dimension was set as a $30 \times 30 \times 30$ Å box. The flexible docking method was used. The flexible region was set as residues near the ligand-binding site. For TTR, the flexible residues were lysine (Lys) 15, leucine (Leu) 17, and Leu 110 in monomer A and Lys 15, Leu 17, glutamic acid (Glu) 54, Leu 110, serine (Ser) 117, threonine (Thr) 119, and valine (Val) 121 in monomer C. For TRα-LBD, the flexible residues were phenylalanine (Phe) 215, Phe 218, isoleucine (Ile) 221, Ile 222, alanine (Ala) 225, arginine (Arg) 228, methionine (Met) 256, Met 259, Ala 263, Arg 266, Leu 292, Ile 299, and histidine (His) 381. For TRβ-LBD, the flexible residues were Phe 269, Phe 272, Ile 275, Ile 276, Arg 282, Met 310, Met 313, Leu 330, Asn 331, Leu 346, Ile 353, His 435, and Phe 455. The binding mode with the lowest binding energy was chosen from 10 independent docking results.

Cell Culture and GH3 Cell Proliferation Assay

GH3 cells were purchased from the Cell Culture Center [Cell Resource Center, Institute of Basic Medical Sciences (IBMS), Chinese Academy of Medical Sciences/Perking Union Medical College (CAMS/PUMS)]. The cells were cultured in Dulbecco's modified Eagle's/F-12 medium (DMEM/F12; Life Technologies; catalog no. 11330032) supplemented with 10% (vol/vol) heat-inactivated fetal bovine serum (FBS; Life Technologies; catalog no. 26400044), and antibiotics (100 U/mL penicillin and 100 μg/mL streptomycin; Life Technologies; catalog no. 15140122). All cells were cultured in a humidified atmosphere composed of 95% air and 5% carbon dioxide at 37°C. The GH3 cell proliferation assay was carried out as described in a previous study (Qin et al. 2019). Briefly, the culture medium was replaced with the test medium [DMEM/F12 without FBS but with bovine insulin (10 mg/mL), ethanolamine (10 mM), sodium selenite (10 ng/mL), bovine serum

Table 1. Hydrophobicity (Log K_{ow}), half maximal inhibitory concentration (IC_{50}), 20% maximal inhibitory concentration (IC_{20}), and relative binding potency (RBP) values obtained from transthyretin (TTR) and thyroid hormone receptor ligand-binding domain (TR-LBD) binding assays; cell proliferation and relative activity (RA) values obtained from the GH3 cell proliferation assay for tetrabromobisphenol A (TBBPA), TBBPA mono-ether structural analogs [TBBPA-mono(glycidyl ether) (TBBPA-MGE), TBBPA-mono(allyl ether) (TBBPA-MAE), and TBBPA-mono(2,3-dibromopropyl ether) (TBBPA-MDBPE)], TBBPA bis-ether derivatives [TBBPA-bis(glycidyl ether) (TBBPA-BGE), TBBPA-bis(allyl ether) (TBBPA-BAE), and TBBPA-bis(2,3-dibromopropyl ether) (TBBPA-BDBPE)], thyroxine (T_4) and triiodothyronine (T_3).

		TTR		TRα-LBD		TRβ-LBD		GH3	
Compound	Log K_{ow}	IC_{50} (μM)	RBP[a]	IC_{20} (μM)	RBP	IC_{20} (μM)	RBP	Effect[b]	RA[c]
TBBPA	7.46	0.2	1.00	1.5	1.00	5.0	1.00	1.1	1.00
TBBPA-MGE	7.31	0.5	0.40	8.0	0.18	6.0	0.83	1.2	1.09
TBBPA-MAE	8.42	0.1	2.00	6.0	0.25	4.0	1.25	1.6	1.45
TBBPA-MDBPE	9.36	1.0	0.20	50.0	0.03	20.0	0.25	4.6	4.18
TBBPA-BGE	7.15	NA[d]	ND	NA	NA	25.0	0.20	ND	ND
TBBPA-BAE	9.37	NA	ND	NA	NA	25.0	0.20	ND	ND
TBBPA-BDBPE	11.26	NA	ND	NA	NA	NA	NA	ND	ND
T_4[e]	—	0.2	1.00	—	—	—	—	—	—
T_3[e]	—	—	—	0.1	15.00	0.05	100.00	—	—

Note: The Log K_{ow} values of the chemicals were obtained from ChemBioDraw. Twenty percent maximal inhibitory concentration (IC_{20}) or half maximal inhibitory concentration (IC_{50}) values were obtained from linear interpolation between two concentrations located at approximately the 20% or 50% inhibition level. —, not applicable; DMSO, dimethyl sulfoxide; NA, not available; ND, not detected; RA, relative activity; RBP, relative binding potency.
[a]RBP compared with TBBPA (set as 1.00).
[b]Effect: GH3 cell proliferation effect compared with the control group (0.1% DMSO), obtained by calculating the absorbance at 450 nm for the compound of interest divided by the absorbance at 450 nm for the control group (0.1% DMSO).
[c]RA compared with TBBPA (set as 1.00).
[d]The addition of the compound led to displacement of the fluorescence probe from TR-LBDs or TTR and did not provide an IC_{20} or IC_{50} value).
[e]The T_4 and T_3 results were obtained from our previous study (Qin et al. 2019).

albumin (500 mg/mL), and human apotransferrin (10 mg/mL)] and incubated for 24 h. The GH3 cells were then seeded in 96-well plates at a density of 5×10^3 cells per well in the test medium. In the GH3 cell proliferation assay, we used three replicate wells per experiment for each group. After 24 h, the cells were exposed to different concentrations of chemicals (0, 0.3, 0.6, 1.2, 2.5, 5, or 10 μM) with or without 2 μM amiodarone (a specific antagonist of TR) to study their effect on cell proliferation. After exposure for 96 h, the proliferative effect was assessed using a Cell Counting Kit-8 (CCK-8) assay (Dojindo; catalog no. CK04). The relative cell proliferation values were calculated by dividing the absorbance at 450 nm of the control group (0.1% DMSO) by that of a cell sample based on the CCK-8 assay. In the present study, we aimed to compare the GH3 cell proliferation activity of TBBPA bis-ether derivatives and TBBPA mono-ether structural analogs with TBBPA by comparing their effects at the same concentration. The relative activity (RA) was calculated by dividing the relative cell proliferation value of TBBPA by that of a TBBPA bis-ether derivative or TBBPA mono-ether structural analog at the concentration of 2.5 μM, which showed no cytotoxicity for all tested chemicals (Figure S1; Table S1). The cytotoxicity was also determined based on the results of the CCK-8 assay. TBBPA and its analogs at concentrations that were not different or had higher absorbance at 450 nm than the control group were considered to have no cytotoxicity. The relative cell proliferation values (compared with the 0.1% DMSO-control group) and RA values (compared with TBBPA, set as 1) are listed in Table 1. To study the antagonistic activity of TBBPA bis-ether derivatives and TBBPA mono-ether structural analogs against TR, cells were exposed to different concentrations of chemicals in the presence of 10 nm T_3. The relative cell proliferation values were calculated by dividing the absorbance of the 10 nM T_3 group at 450 nm by that of a cell sample based on the CCK-8 assay.

Detection of Intracellular TBBPA-MDBPE and TBBPA

GH3 cells ($\sim 5 \times 10^5$ cells) were seeded in 25-cm^2 flasks in test medium. After 12 h, TBBPA-MDBPE or TBBPA was added to the medium to obtain a final concentration of 2.5 μM, which showed no cytotoxicity for these two chemicals (Figure S1C,D). After 24 h, the cells were harvested by trypsin-EDTA (Life Technologies). The cells were washed four times with phosphate-buffered saline buffer [137 mM sodium chloride, 2.7 mM KCl, 10 mM disodium phosphate, and 1.8 mM monopotassium phosphate, pH 7.4] by centrifuging the cells at 4,000 rpm for 5 min at 4°C. Then, the cell density was counted by a Countess cell counter (Life Technologies). Intracellular TBBPA-MDBPE and TBBPA were extracted, and their amounts were detected according to the methods below.

Sample pretreatment. The sample pretreatment method was performed as described in a previous study with slight modifications (Yu et al. 2016). In brief, the cell pellet (approximately 5×10^5 cells) of each sample was mixed with 2 mL of hydrochloric acid (6 mol/L) and 6 mL of dimethylcarbinol. Next, 15 mL of a mixture of hexane and methyl tertiary butyl ether (1:1, vol/vol) was added to extract the chemicals from the cells by applying an ultrasonic cell disrupter for 5 min. The supernatant was collected after centrifugation at 4,000 rpm for 15 min. The above ultrasonic extraction process was repeated twice, and the supernatants were collected and mixed together. Next, 20 mL of 1% KCl and 20 mL of water were added to the collected extraction solution to precipitate the proteins and impurities. Anhydrous sodium sulfate was added to remove water. The extraction solution was then removed gently with a rotary evaporator and nitrogen blowing. The target compounds were then reconstituted in 1.5 mL of methanol and introduced to a HybridSPE-Phospholipid cartridge (30 mg, 1 mL; Supelco) for further purification. Finally, 50 ng of Deuterated-labeled TBBPA (D_{10}-TBBPA) was spiked as an internal standard and redissolved in 1 mL of methanol before analysis.

Liquid chromatography–electrospray ionization–tandem mass spectrometry analysis. The amount of TBBPA-MDBPE or TBBPA was detected by a high-performance liquid chromatography (HPLC; Waters; 2695) tandem mass spectrometry system (MS/MS; Quattro Premier XE; Waters), with electrospray ionization (ESI) as the ion source (LC-ESI-MS/MS). A 20-μL sample was injected into the chromatographic column (Zorbax® ODS; 150 × 3 mm, 5 μm; Agilent), and the compounds were separated through gradient elution. Methanol and ultrapure water with 1 mM ammonium acetate were used as the mobile phases at a flow rate of 0.6 mL/min. Both TBBPA-MDBPE and TBBPA were detected in negative electrospray ionization mode, and the identification of compounds was performed by comparing the

retention times and selected ion pairs with the corresponding standard compounds.

Quantification and method validation. The concentrations of TBBPA-MDBPE and TBBPA were quantified using internal standards. Calibration curves were established based on 10 points (0.1, 0.5, 1, 5, 10, 25, 50, 100, 250, and 500 ng/mL), and the correlation coefficients (R^2) were >0.9. Three different levels of TBBPA-MDBPE and TBBPA (10, 100, and 1,000 ng/mL, $n = 3$) were added to the blank cell matrix to examine the recovery rate of the sample pretreatment method. The LOD and limit of quantification (LOQ) were determined using signal-to-noise ratios of 3 and 10, respectively. The LOD values for TBBPA-MDBPE and TBBPA were 0.10 ng/mL and 0.13 ng/mL, respectively. The LOQ values for TBBPA-MDBPE and TBBPA were 0.32 ng/mL and 0.43 ng/mL, respectively. All cell samples were analyzed in triplicate, and the same unspiked samples were prepared in the same batch as the blank controls.

Statistical Analysis

All experiments were conducted in triplicate. The data are expressed as the mean value plus or minus the standard deviation ($n = 3$). The p-values of the experimental data were analyzed using one-way analysis of variance tests, followed by a least significant difference multiple comparisons test (IBM SPSS Statistics 20). A p-value of <0.05 was considered to be statistically significant.

Results

Interaction of TBBPA Mono-Ether Structural Analogs with Human TH Transport Proteins

We first studied the potential TH system–disrupting effects of TBBPA mono-ether structural analogs via the mechanism of TH transport disruption. We quantitatively determined the binding potencies of TBBPA, three TBBPA mono-ether structural analogs (TBBPA-MGE, TBBPA-MAE, and TBBPA-MDBPE) and three TBBPA bis-ether derivatives (TBBPA-BGE, TBBPA-BAE, TBBPA-BDBPE) with two major human transport proteins, TTR and TBG. As shown in Figure 2A–C, Table S2, Figure S2, and Table S3, all of the tested TBBPA mono-ether structural analogs bound to TTR but not to TBG. They bound to TTR with IC_{50} values ranging from 0.1 μM (57 μg/L, TBBPA-MAE) to 1.0 μM (736 μg/L, TBBPA-MDBPE), with TBBPA-MAE showing the highest binding potency (Table 1). The TTR-binding potencies of TBBPA-MGE and TBBPA-MDBPE were approximately 2- or 5-fold lower than those of the natural ligand T_4, whereas TBBPA-MAE showed 2-fold higher TTR-binding potency than T_4 (Table 1). As shown in Figure 2D and Figure S2, TBBPA bound to TTR with an IC_{50} value of approximately 0.2 μM, but it did not bind to TBG. Three TBBPA bis-ether derivatives bound TTR with IC_{50} values >50 μM (Figure 2E–G; Table 1). They also did not bind to TBG (Figure S2). The tested chemicals showed the following relative TTR-binding potencies: TBBPA-MAE > TBBPA > TBBPA-MGE > TBBPA-MDBPE > TBBPA-BGE ≈ TBBPA-BAE ≈ TBBPA-BDBPE (Table 1).

Based on the above competitive binding assays, we demonstrated that the three tested TBBPA bis-ether derivatives displayed very low or negligible binding potencies to TH transport proteins. In contrast, the TBBPA mono-ether structural analogs bound to TTR, and one chemical displayed a higher binding potency than TBBPA (TBBPA-MAE; 2-fold greater). We further used molecular docking analysis to simulate the binding modes of TBBPA mono-ether structural analogs with TTR. The identified binding sites of these chemicals on TTR are shown in Figure 3A–C, whereas the binding scores and interactions of these chemicals with TTR are shown in Table S4 and Figure S3, respectively. We found that the order of the docking scores (a higher score means higher potential binding potency) (Table S4) and the observed binding potencies (Table 1) of these chemicals were consistent with each other. As shown in Figure 3A–C, TBBPA-MGE and TBBPA-MDBPE fit into TTR with their OH groups oriented toward the entrance of the protein, whereas their derivatized groups were positioned toward the inner part of the binding pocket. TBBPA-MAE fit into TTR in the opposite orientation, with its OH group oriented toward the inner part of the binding pocket (Figure 3B). TBBPA was also included in the docking analysis for comparison. We found that the binding sites of the TBBPA mono-ether structural analogs in TTR were similar to those of TBBPA (Figure 3A–C). The identical moieties of these chemicals—including two benzene rings, four bromine atoms, two methyl groups, and one OH group—resided in similar sites, whereas the residual differently derivatized moieties of the TBBPA mono-ether structural analogs resided at the site where the other OH group of TBBPA was located (Figure 3A–C). As shown in Table S4, the interactions, especially the hydrophobic interactions, between the TBBPA mono-ether structural analogs and TTR were also similar to those between TBBPA and TTR. Based on the above results, TBBPA mono-ether structural analogs and TBBPA likely bind to human TTR through a similar mechanism, and the derivatized groups were shown to modulate TTR-binding potency.

Interaction of TBBPA Mono-Ether Structural Analogs with Human TR-LBDs

We then studied the potential TH system–disrupting effects of the TBBPA mono-ether structural analogs via the mechanism of interaction with TR in TH-responsive cells. First, we explored the possibility of direct binding of these chemicals with TRs. We quantitatively determined the binding potencies of TBBPA, the three TBBPA mono-ether structural analogs and the three TBBPA bis-ether derivatives with two subtypes of human TR-LBDs, TRα-LBD and TRβ-LBD. As shown in Figure 4A–C, Table S5, and Table 1, TBBPA mono-ether structural analogs bound TRα-LBD with IC_{20} values ranging from 6.0 μM (3.4 mg/L, TBBPA-MAE) to 50.0 μM (36.8 mg/L, TBBPA-MDBPE), with TBBPA-MAE showing the highest binding potency. These compounds bound TRβ-LBD with IC_{20} values ranging from 4.0 μM (2.3 mg/L, TBBPA-MAE) to 20.0 μM (14.7 mg/L, TBBPA-MDBPE), again with TBBPA-MAE showing the highest binding potency (Table 1; Figure S4A–C; Table S6). The TR-LBD binding potencies of these TBBPA mono-ether structural analogs were approximately 60- to 500-fold lower than those of the natural ligand T_3 (Table 1). As shown in Figure 4D, Table 1, and Figure S4D, TBBPA bound to TRα-LBD and TRβ-LBD with IC_{20} values of 1.5 μM and 5.0 μM, respectively. The three bis-ether derivatives bound to TRα-LBD with IC_{20} values >50 μM; they bound TRβ-LBD with IC_{20} values of 20 μM to >50 μM (Figure 4E–G; Table 1; Figure S4E–G). The relative TRα-LBD binding potencies of all the tested chemicals were as follows: TBBPA > TBBPA-MAE > TBBPA-MGE > TBBPA-MDBPE > TBBPA-BGE ≈ TBBPA-BAE ≈ TBBPA-BDBPE (Table 1). For TRβ-LBD, the relative binding potencies were as follows: TBBPA-MAE > TBBPA > TBBPA-MGE > TBBPA-MDBPE > TBBPA-BGE ≈ TBBPA-BAE > TBBPA-BDBPE (Table 1).

We also used molecular docking analysis to simulate the binding modes of the TBBPA mono-ether structural analogs with the TR-LBDs. The identified binding sites of these chemicals in TRα-LBD and TRβ-LBD are shown in Figure 3D–F and Figure S5, respectively. The binding scores and interactions of these chemicals with TRα-LBD and TRβ-LBD are shown in Tables S7 and S8 and Figures S6 and S7, respectively. The docking score order (Tables S7 and S8) and the observed binding potencies

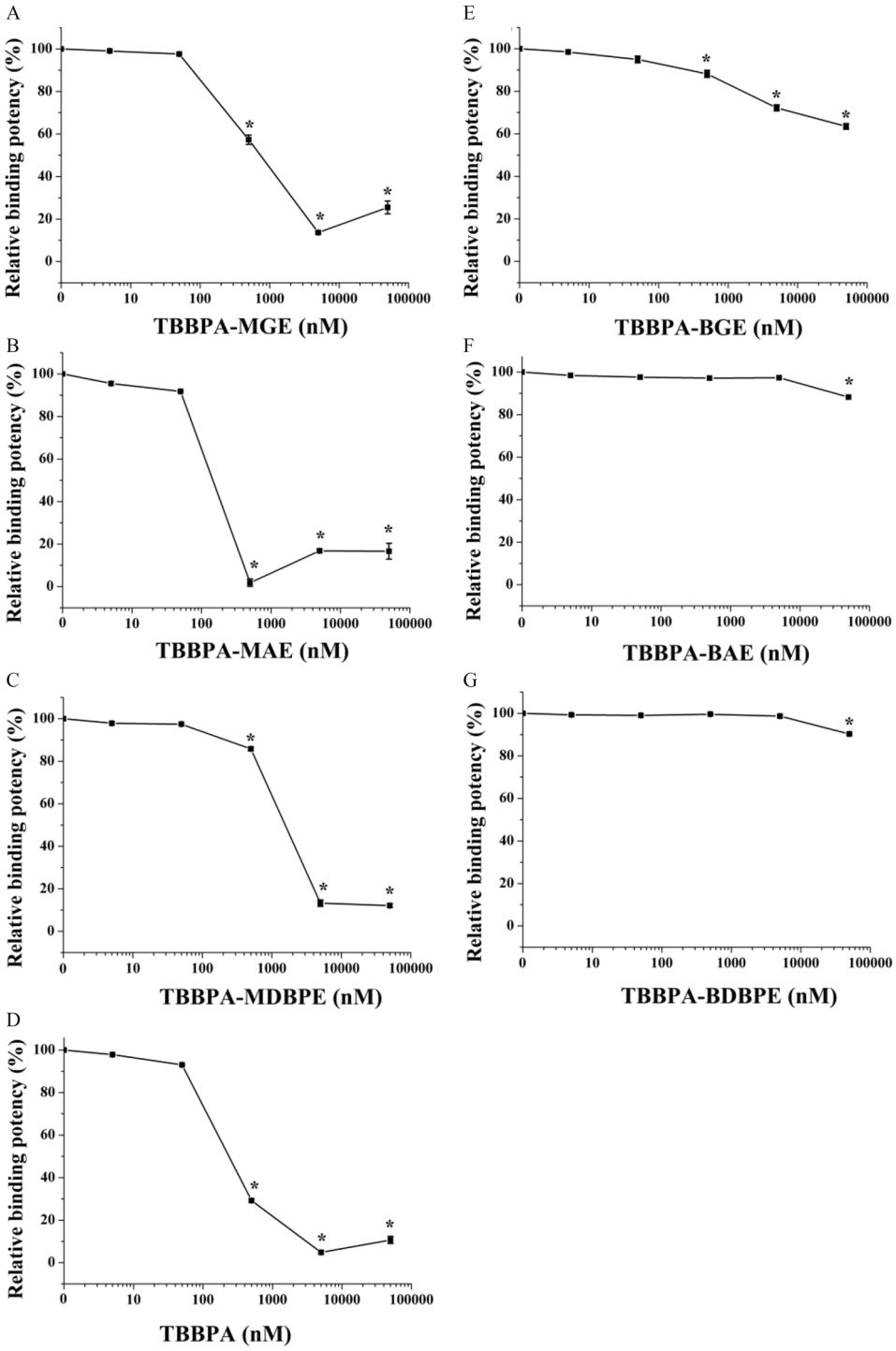

Figure 2. Competitive binding curves of the tetrabromobisphenol A (TBBPA) mono-ether structural analogs [(A) TBBPA-mono(glycidyl ether) (TBBPA-MGE), (B) TBBPA-mono(allyl ether) (TBBPA-MAE), and (C) TBBPA-mono(2,3-dibromopropyl ether) (TBBPA-MDBPE)], (D) TBBPA, the TBBPA bis-ether derivatives [(E) TBBPA-bis(glycidyl ether) (TBBPA-BGE), (F) TBBPA-bis(allyl ether) (TBBPA-BAE), and (G) TBBPA-bis(2,3-dibromopropyl ether) (TBBPA-BDBPE)] with transthyretin. Three replicate wells were included for each group in a 96-well plate. Error bars represent the standard deviation of three replicates. $^{*}p < 0.05$, compared with the control group (1% dimethyl sulfoxide). The *p*-values of the experimental data were analyzed using a one-way analysis of variance, followed by a least significant difference multiple comparisons test (IBM SPSS Statistics 20). See the summary data in Table S3.

(Table 1) of these chemicals with the TR-LBDs were consistent with each other. As shown in Figure 3D,F, TBBPA-MGE and TBBPA-MDBPE fit into TRα-LBD with their OH groups oriented toward the entrance of the receptor, whereas their derivative groups were positioned toward the inner part of the binding pocket. TBBPA-MAE fit into TRα-LBD in an opposite orientation, with its OH group oriented toward the inner part of the binding pocket (Figure 3E). Similarly, TBBPA-MGE and TBBPA-MDBPE fit into TRβ-LBD with their OH groups oriented toward the entrance of the receptor, whereas TBBPA-MAE with its OH group oriented toward the inner part of the binding pocket (Figure S5). TBBPA was also docked in the TR-LBDs for comparison. We found that the TBBPA mono-ether structural analogs had similar binding sites as TBBPA in the TR-LBDs (Figure 3D–F; Figure S5).

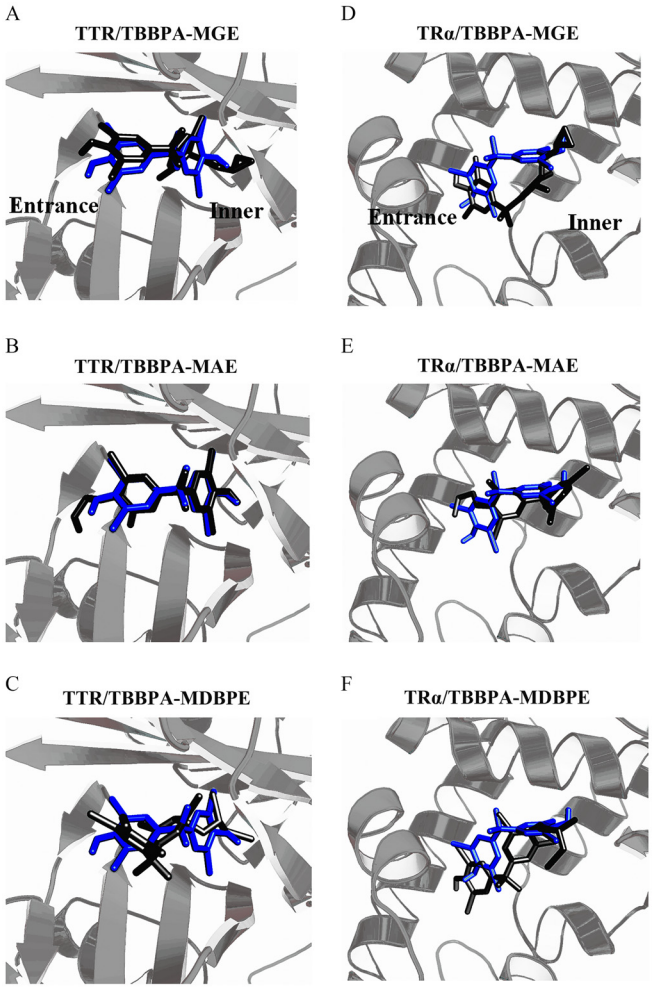

Figure 3. Overlay of the binding modes of the tetrabromobisphenol A (TBBPA) mono-ether structural analogs [(A,D) TBBPA-mono(glycidyl ether) (TBBPA-MGE), (B,E) TBBPA-mono(allyl ether) (TBBPA-MAE), and (C,F) TBBPA-mono(2,3-dibromopropyl ether) (TBBPA-MDBPE)] with TBBPA in (A,B,C) human transthyretin (TTR) and (D,E,F) the thyroid hormone receptor α-ligand binding domain (TRα-LBD). The proteins are shown in gray. TBBPA is shown in blue. The TBBPA mono-ether structural analogs are shown in black.

TBBPA Mono-Ether Structural Analogs Induced GH3 Cell Proliferation via TR

Here, we investigated the effects of individual exposure with TBBPA, three TBBPA mono-ether structural analogs, or three TBBPA bis-ether derivatives on GH3 cell proliferation. As shown in Figure 5A–C and Table S9, the TBBPA mono-ether structural analogs induced GH3 proliferation with the highest activities ranging from 252% to 464% and the lowest effective concentrations (LOECs) ranging from 0.3 μM (220 μg/L, TBBPA-MDBPE) to 2.5 μM (1.4 mg/L, TBBPA-MGE). TBBPA induced GH3 cell proliferation with the highest activity of 137% and a LOEC of 2.5 μM (Figure 5D). The three bis-ether derivatives induced GH3 cell proliferation with the highest activities ranging from 116% to 125% and LOECs of 5.0 μMor 10.0 μM (Figure 5E–G). Intriguingly, among the TBBPA structural analogs and TBBPA, TBBPA-MDBPE showed distinctly higher activity. To confirm that TR was involved in the GH3 cell proliferation effect, we introduced a specific TR antagonist. When the cells were co-exposed to 2.0 μM amiodarone, the effects induced by the TBBPA mono-ether structural analogs were significantly ($p < 0.05$) inhibited (Figure 5A–C; Table S9). At the same concentration (2.5 μM), the relative GH3 cell proliferation activities of the tested chemicals were as follows: TBBPA-MDBPE > TBBPA-MAE > TBBPA-MGE > TBBPA > TBBPA-BGE ≈ TBBPA-BAE ≈ TBBPA-BDBPE (Table 1).

TBBPA Mono-Ether Structural Analogs Enhanced T_3-Induced GH3 Cell Proliferation

We also investigated the effects of the tested chemicals on GH3 cell proliferation when co-exposed with 10 nM T_3 (the saturation concentration that induced the highest GH3 cell proliferation effect) (Qin et al. 2019). As shown in Figure 6A–C and Table S10, when the cells were co-exposed to T_3, the three TBBPA mono-ether structural analogs enhanced the T_3-induced GH3 cell proliferation effects by 31% to 43%, with LOECs ranging from 0.3 μM (220 μg/L, TBBPA-MDBPE) to 1.2 μM (0.7 mg/L, TBBPA-MGE). TBBPA also enhanced the T_3-induced GH3 cell proliferation effect by 20%, with a LOEC of 2.5 μM (Figure 6D). Regarding the three bis-ether derivatives, TBBPA-BGE and TBBPA-BAE inhibited the T_3-induced GH3 cell proliferation effect by approximately 80% and 60%, respectively (Figure 6E,F), whereas TBBPA-BDBPE showed no effect (Figure 6G).

Comparison of the Membrane Transportation Ability of TBBPA-MDBPE and TBBPA in GH3 Cells

Based on the above results, we found that TBBPA-MDBPE showed much higher (4.18-fold) GH3 cell proliferation activity than TBBPA (Figure 5C,D and Table 1). Given that TBBPA-MDBPE has a distinctly different hydrophobicity (Log K_{ow}) from TBBPA (Table 1), we hypothesized that its higher GH3 cell proliferation activity might be due to its higher membrane transportation ability. To test this hypothesis, we measured the intracellular amounts of TBBPA-MDBPE and TBBPA in GH3 cells after exposure to the same concentration (2.5 μM) of these two compounds. We determined the intracellular amounts of TBBPA-MDBPE and TBBPA in GH3 cells at the same exposure concentration of 2.5 μM. At this concentration, TBBPA showed no difference from the control group (Figure S1D), whereas TBBPA-MDBPE showed a higher absorbance at 450 nm than the control group (Figure S1C), suggesting that these two chemicals had no cytotoxicity to GH3 cells at a concentration of 2.5 μM. The cell membrane should remain intact when the cells are exposed to these chemicals at this concentration, and the amount of chemicals in GH3 cells was probably related to their membrane transportation ability. We used HPLC and MS/MS to detect the concentrations of TBBPA-MDBPE and TBBPA in the tested samples. The LOD values for TBBPA-MDBPE and TBBPA were 0.10 ng/mL and 0.13 ng/mL, respectively (Table 2). The LOQ values for TBBPA-MDBPE and TBBPA were 0.32 ng/mL and 0.43 ng/mL, respectively (Table 2). The recovery rates were in the range of 68% to 80% and 76% to 120% for TBBPA-MDBPE and TBBPA, respectively (Table 2). The above results demonstrated the accuracy of the sample pretreatment and the chemical analysis methods. As shown in Table 2, after 24 h of exposure, the amounts of TBBPA-MDBPE and TBBPA in 5×10^5 GH3 cells were approximately 2,013.56 ng (2,733.5 pmol) and 14.10 ng (25.9 pmol), respectively. The results showed that the amount of TBBPA-MDBPE in the GH3 cells was approximately 105-fold higher than that of TBBPA when the cells were exposed to the same concentration (2.5 μM). This demonstrated that TBBPA-MDBPE had a much higher membrane transportation ability than TBBPA.

Discussion

In mammals, TH synthesis and secretion are finely modulated by the hypothalamic–pituitary–thyroid axis and regulate normal

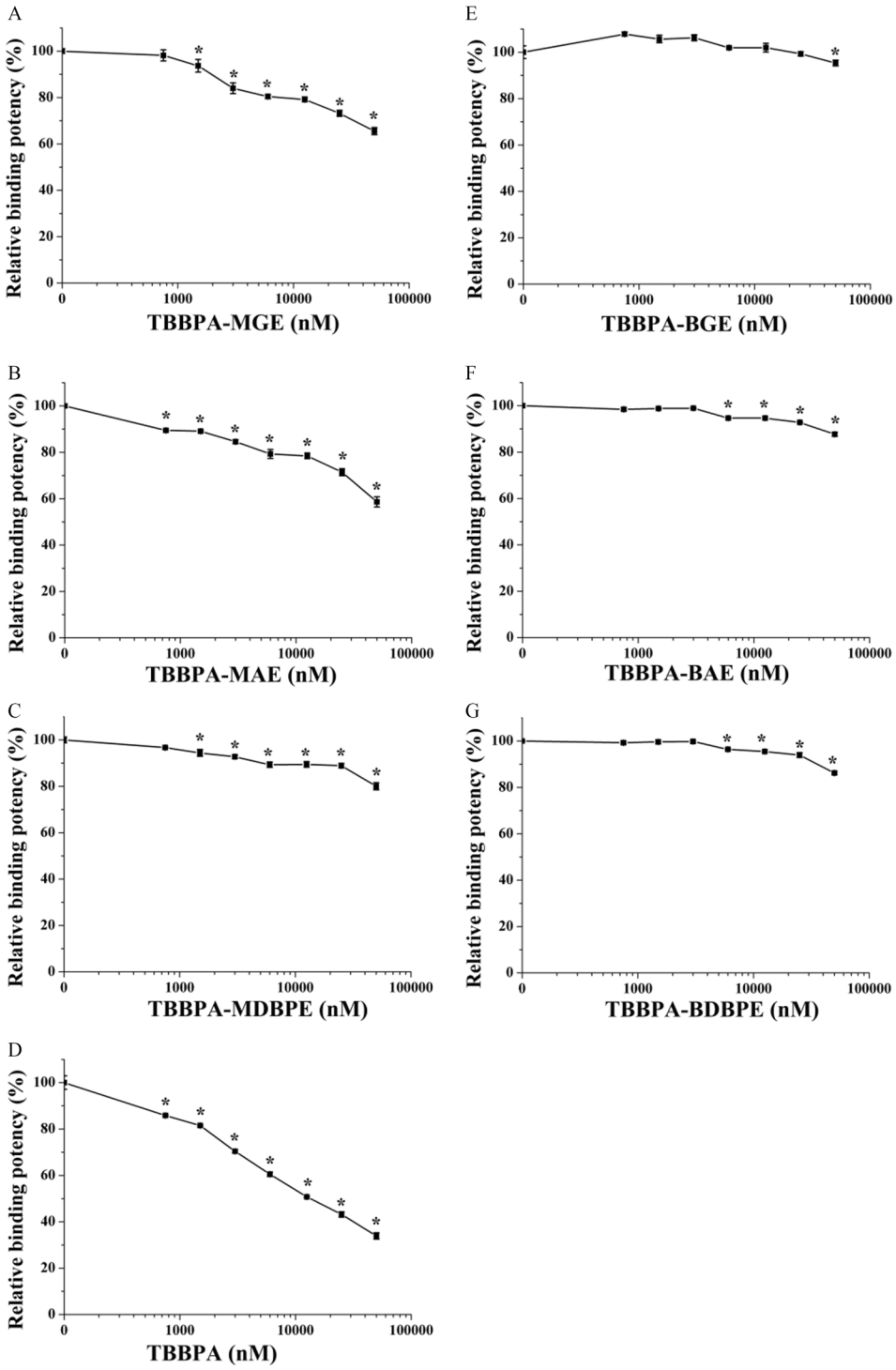

Figure 4. Competitive binding curves of the tetrabromobisphenol A (TBBPA) mono-ether structural analogs [(A) TBBPA-mono(glycidyl ether) (TBBPA-MGE), (B) TBBPA-mono(allyl ether) (TBBPA-MAE), and (C) TBBPA-mono(2,3-dibromopropyl ether) (TBBPA-MDBPE)], (D) TBBPA, and the TBBPA bis-ether derivatives [(E) TBBPA-bis(glycidyl ether) (TBBPA-BGE), (F) TBBPA-bis(allyl ether) (TBBPA-BAE), and (G) TBBPA-bis(2,3-dibromopropyl ether) (TBBPA-BDBPE)] with the thyroid hormone receptor α-ligand binding domain (TRα-LBD). Three replicate wells were included for each group in a 96-well plate. Error bars represent the standard deviation of three replicates. $^{*}p < 0.05$, compared with the control group (1% dimethyl sulfoxide). The *p*-values of the experimental data were analyzed using a one-way analysis of variance, followed by a least significant difference multiple comparisons test (IBM SPSS Statistics 20). See the summary data in Table S5.

blood circulating TH homeostasis (Mendoza and Hollenberg 2017). Various endocrine-disrupting chemicals have the potential to disturb TH homeostasis via competitive binding with the TH transport proteins TTR and/or TBG in the blood (Meerts et al. 2000; Ren and Guo 2012). Previously, Meerts et al. (2000) used a ^{125}I-T_4 radio ligand displacement assay to demonstrate that TBBPA bound to human TTR. Here, by using a human TH transport protein competitive binding assay that was established in our previous study (Ren and Guo 2012), we also demonstrated the TTR-binding potential of TBBPA (Figure 2D). Similar to

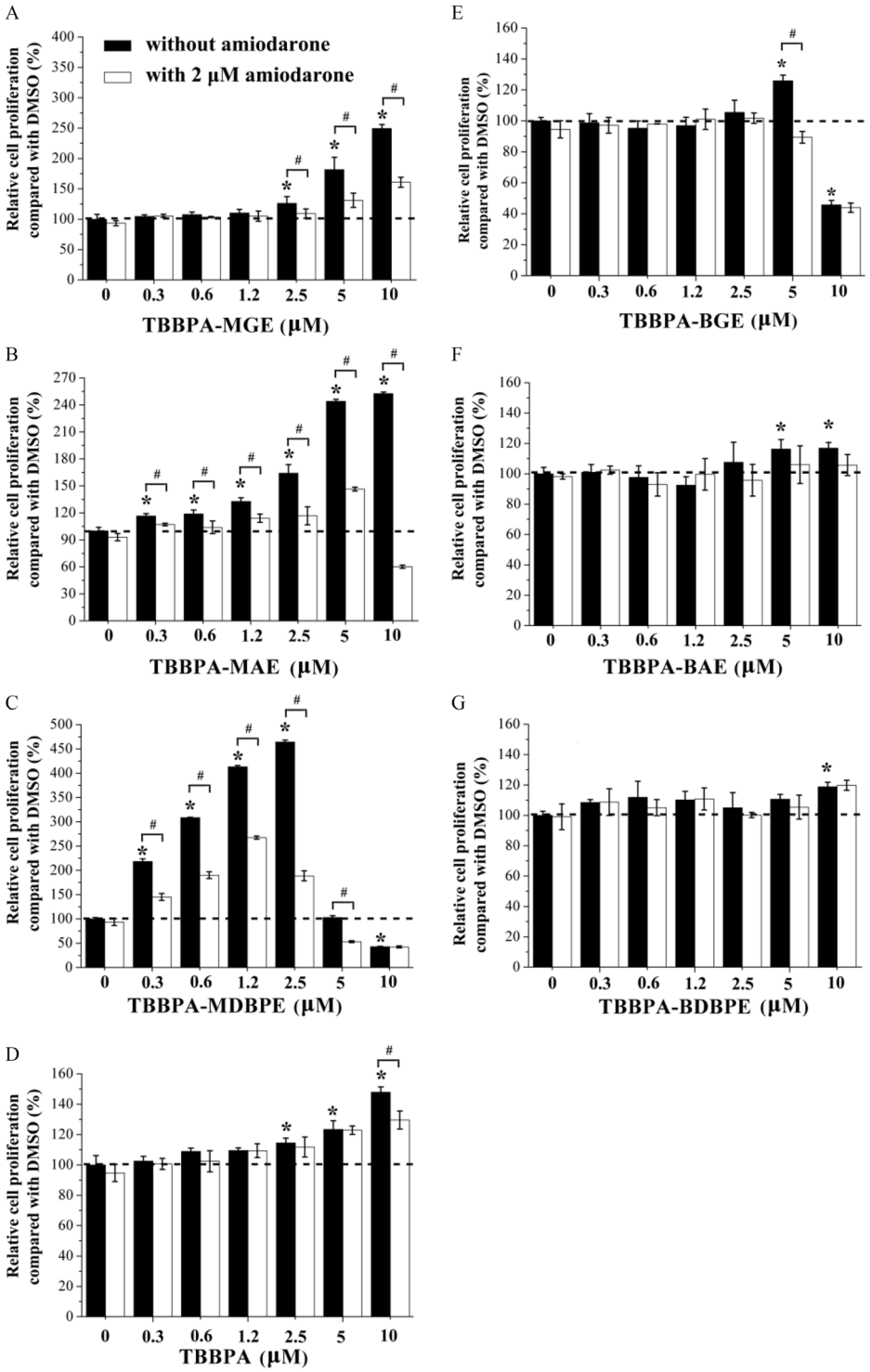

Figure 5. Agonistic activity of the tetrabromobisphenol A (TBBPA) mono-ether structural analogs [(A) TBBPA-mono(glycidyl ether) (TBBPA-MGE), (B) TBBPA-mono(allyl ether) (TBBPA-MAE), and (C) TBBPA-mono(2,3-dibromopropyl ether) (TBBPA-MDBPE)], (D) TBBPA, and the TBBPA bis-ether derivatives [(E) TBBPA-bis(glycidyl ether) (TBBPA-BGE), (F) TBBPA-bis(allyl ether) (TBBPA-BAE), and (G) TBBPA-bis(2,3-dibromopropyl ether) (TBBPA-BDBPE)] determined by the GH3 cell proliferation assay. GH3 cells were treated with different concentrations of the tested chemicals in the presence or absence of 2.0 μM amiodarone. Three replicated wells were included for each group in a 96-well plate. Error bars represent the standard deviation of three replicates. Relative cell proliferation values were calculated by dividing the absorbance value at 450 nm of the control group (0.1% DMSO) by that of each cell sample based on the Cell Counting Kit-8 assay. $^{*}p < 0.05$, compared with cell samples of the control group (0.1% DMSO). $^{\#}p < 0.05$, compared with cell samples treated without 2.0 μM amiodarone. The p-values of the experimental data were analyzed using a one-way analysis of variance, followed by a least significant difference multiple comparisons test (IBM SPSS Statistics 20). See the summary data in Table S9. Note: DMSO, dimethyl sulfoxide.

TBBPA, TBBPA mono-ether structural analogs bound to human TTR (Figure 2A–C). We further revealed that TBBPA mono-ether structural analogs specifically bound to TTR at the TH binding site based on the site-specific fluorescence probe F-T_4. Moreover, the TTR-binding potency of TBBPA-MAE was higher than that of TBBPA and even higher than that of the natural

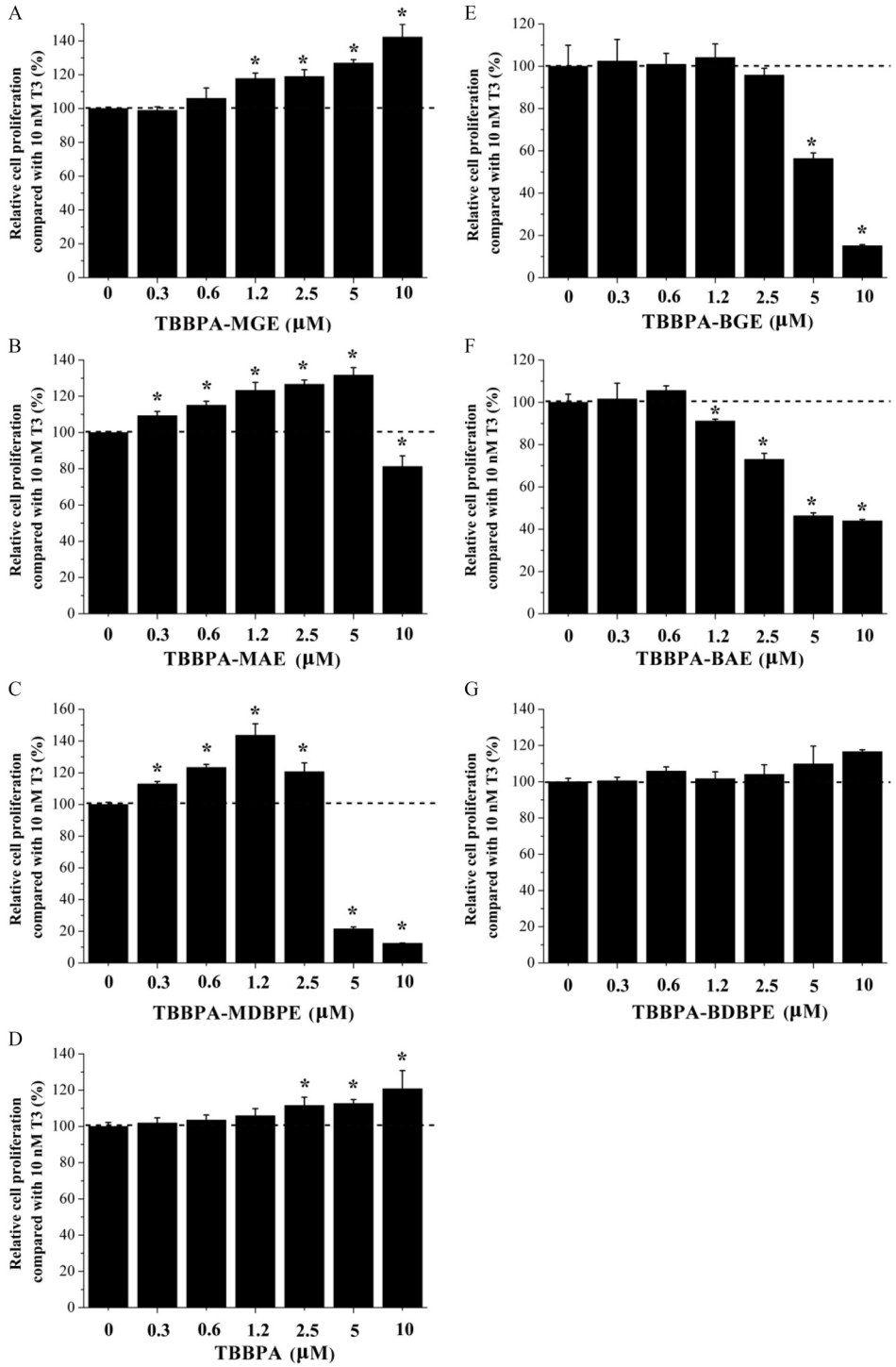

Figure 6. Antagonistic activity of the tetrabromobisphenol A (TBBPA) mono-ether structural analogs [(A) TBBPA-mono(glycidyl ether) (TBBPA-MGE), (B) TBBPA-mono(allyl ether) (TBBPA-MAE), and (C) TBBPA-mono(2,3-dibromopropyl ether) (TBBPA-MDBPE)], (D) TBBPA, the TBBPA bis-ether derivatives [(E) TBBPA-bis(glycidyl ether) (TBBPA-BGE), (F) TBBPA-bis(allyl ether) (TBBPA-BAE), and (G) TBBPA-bis(2,3-dibromopropyl ether) (TBBPA-BDBPE)] determined by GH3 cell proliferation assay. GH3 cells were treated with different concentrations of the tested chemicals in the presence of 10 nM triiodothyronine (T_3). Three replicate wells were included for each group in a 96-well plate. Error bars represent the standard deviation of three replicates. The relative cell proliferation values were calculated by dividing the absorbance value at 450 nm of the 10 nm T_3 group by that of each cell sample based on the Cell Counting Kit-8 assay. $^{*}p < 0.05$, compared with the group treated with 10 nm T_3. The p-values of the experimental data were analyzed using a one-way analysis of variance, followed by a least significant difference multiple comparisons test (IBM SPSS Statistics 20). See the summary data in Table S10.

ligand T_4 (Table 1), indicating the strong unexpected TH transport-disrupting potential of this chemical. TTR is critical in the transport of TH across the blood–brain barrier and plays an important role in TH action in the brain (Zheng et al. 2001). Therefore, binding of these chemicals to TTR may not only affect blood circulating TH homeostasis but also decrease the availability of TH specifically in the brain. Moreover, it has also been demonstrated that TTR mediates the transport of environmental pollutants into the placenta (Meerts et al. 2002). The binding of TBBPA mono-ether structural analogs to TTR might also

Table 2. Limit of detection (LOD), limit of quantification (LOQ), recovery rates at different concentrations, and the determined intracellular amount of TBBPA-mono(2,3-dibromopropyl ether) (TBBPA-MDBPE) and tetrabromobisphenol A (TBBPA).

Results	TBBPA-MDBPE	TBBPA
LOD (ng/mL)	0.10	0.13
LOQ (ng/mL)	0.32	0.43
Recovery at 10 ng/mL (%)	68 ± 27	76 ± 18
Recovery at 100 ng/mL (%)	70 ± 8	104 ± 19
Recovery at 1,000 ng/mL (%)	80 ± 10	120 ± 12
Intracellular amount (ng)	$2{,}013.56 \pm 91.86$	14.10 ± 2.50

mediate the translocation of these chemicals across the placental barrier and lead to exposure to the fetus.

Various TBBPA structural analogs, including TBBPA bis-ether derivatives, have been designed and synthesized as BFRs with the aim of enhancing some desired properties, such as safety to human health (Alaee et al. 2003). Here, we demonstrated that the TTR-binding potencies of the TBBPA mono-ether structural analogs were higher than those of the bis-ether derivatives (Table 1), which adds important information regarding the effects of the OH derivatized groups on the interaction between TBBPA structural analogs and TTR. Moreover, these results showed that the TBBPA mono-ether structural analogs, which occur as by-products and transformation products in the environment, displayed greater potential TH-disruptive effects than TBBPA bis-ether derivatives.

Molecular docking showed that, like TBBPA, the TBBPA mono-ether structural analogs also fit into the ligand-binding pocket of TTR, and they had similar binding modes (Figure 3; Table S4). In view of the similar binding sites of the three tested TBBPA mono-ether structural analogs in the TTR, the different protein binding potencies could be explained by the variations in the interactions between the differently derivatized groups and the protein. For TTR, TBBPA-MAE (with an allyl group having a moderate size and Log K_{ow} compared with the other two chemicals) displayed higher binding potency than the other two TBBPA mono-ether structural analogs. Compared with the other two chemicals, TBBPA-MAE might maintain a better balance between hydrophobic effects and steric hindrance in the TTR ligand-binding pocket, which in turn leads to its higher binding potency.

TR, as a nuclear hormone receptor, has been demonstrated to regulate the expression of various target genes responsible for development and energy homeostasis (Astapova et al. 2008; Morte et al. 2002). Disruption of the normal function of TR in TH-responsive cells could lead to various adverse effects such as neurotoxicity and metabolic disorders (Heindel et al. 2017; Schreiber et al. 2010). Both apo-TRs (receptors without ligand) and ligand-bound TRs could regulate target gene expression. In the absence of ligands, apo-TRs could heterodimerize with retinoid-X receptor (RXR) and recruit the binding of nuclear corepressors, which ultimately repress or silence basal target gene expression (Mendoza and Hollenberg 2017). Binding of T_3 to TRs could alter the conformations of TRs in such a way that the corepressor complex is replaced by a coactivator, which in turn activates gene expression (Harvey and Williams 2002). Therefore, for environmental pollutants, both direct binding to apo-TRs and competitive binding to T_3-bound TRs could interfere with the normal function of TRs.

Previously, Kollitz et al. (2018) used a ^{125}I-T_3 radio ligand displacement assay to demonstrate that TBBPA bound to human TRβ-LBD. Here, by using human TR-LBD competitive binding assays, we also demonstrated the binding of TBBPA to human TR-LBDs. We further demonstrated that, like TBBPA, TBBPA mono-ether structural analogs bound to both human TRα-LBD and TRβ-LBD (Figure 4A–C; Figure S4A–C). The site-specific fluorescence probe F-T_3 demonstrated the specific binding of TBBPA mono-ether structural analogs to human TR-LBDs at the TH binding sites. Molecular docking showed that the mono-ether structural analogs fit into ligand-binding pockets of TR-LBDs (Figure 3; Tables S7 and S8), which supported the binding of these chemicals to TRs. Based on the results of the competitive binding assay and molecular docking, we demonstrated the binding ability of TBBPA mono-ether structural analogs to the TR-LBDs (Figure 4A–C) and even had high potentials similar to that of the natural TH T_3.

It has been demonstrated that activation of TR in rat pituitary tumor GH3 cells regulates cell proliferation activity (Gutleb et al. 2005). Therefore, the GH3 cell proliferation assay has been widely applied to study the cellular TR-disrupting potencies of pollutants (Kitamura et al. 2002; Qin et al. 2019). Our results showed that the TBBPA mono-ether structural analogs induced GH3 cell proliferation, and these effects were inhibited by the specific TR antagonist amiodarone (Figure 5A–C). In addition to inducing GH3 cell proliferation after individual exposure, TBBPA and the TBBPA mono-ether structural analogs further enhanced T_3-induced GH3 cell proliferation (Figure 6A–D), which is in line with the results of a previous study on TBBPA (Kitamura et al. 2002). In some studies of other pollutants, such as tributyltin and triphenyltin, it was suggested that these chemicals might enhance T_3-induced TR activation in GH3 cells through binding to RXR (Mengeling et al. 2016, 2018). Therefore, the role of TBBPA and TBBPA mono-ether structural analogs binding to other receptors in the enhancement of T_3-induced GH3 cell proliferation cannot be excluded, which warrants further detailed investigation.

Notably, we found that one of the tested TBBPA mono-ether structural analogs, TBBPA-MDBPE, showed much higher GH3 cell proliferation activity than TBBPA (Figure 5C,D; Table 1). This did not appear to be correlated with the results obtained from the TR-LBDs binding assays and molecular docking assays, which showed that TBBPA-MDBPE had much weaker binding potencies to the TR-LBDs than TBBPA (Table 1). By using the developed LC-ESI-MS/MS method, we demonstrated that the intracellular amount of TBBPA-MDBPE was 105-fold higher than that of TBBPA, suggesting that TBBPA-MDBPE has a higher ability to transport across the cell membrane into GH3 cells than TBBPA (Table 2). The proper hydrophobicity of TBBPA-MDBPE might lead to its higher membrane transportation ability, which could then lead to its higher potential to stimulate GH3 cell proliferation. The bioavailability of a pollutant, which normally refers to a complex *in vivo* outcome—including absorption, distribution, metabolism, and excretion—is relevant to its toxicity (Bradham et al. 2018). The membrane transportation ability of a pollutant, which is directly correlated to its hydrophobicity, is one of the factors affecting bioavailability (Semple et al. 2004). Therefore, the membrane transportation ability of TBBPA-MDBPE to cells is a critical factor that determines its higher potential to stimulate GH3 cell proliferation.

The presence of TBBPA derivatives and analogs in the environment has attracted a large amount of attention, especially regarding their potential toxicity due to their unique structures. Previously, a few studies have discussed the endocrine-disrupting potency, neurotoxicity, and preadipocytes of TBBPA and TBBPA analogs (Eng et al. 2019; Liu et al. 2016, 2020; Pullen et al. 2003). However, detailed molecular interactions have not been elucidated, leaving the mechanism underlying the different toxicities of TBBPA analogs remaining elusive. Here, in terms of TH disrupting potency, based on *in vitro* and *in silico* methods, we demonstrated exact interaction sites between the chemicals and associated receptors. The TBBPA mono-ether

structural analogs also showed higher membrane transportation ability than TBBPA, which determined the higher potential to stimulate the proliferation of GH3 cells. Taken together, our results showed a possible molecular mechanism underlying the higher TH disrupting potency of TBBPA mono-ether structural analogs.

The exposure sources of TBBPA and TBBPA analogs are contaminated environmental matrices, food, and commercial products containing TBBPA (Abou-Elwafa Abdallah 2016; Liu et al. 2015, 2016; Qu et al. 2011). Recently, TBBPA in human breast milk in the general population in China was reported to be approximately at 1.57 ng/g lipid weight (Huang et al. 2020). The TBBPA concentration in human serum samples collected from the general population in Korea was approximately 45.6 ng/g lipid weight ($\sim$0.5 nM) (Kim and Oh 2014). To date, because of the lack of commercial standards, there are no data about the exposure levels of TBBPA derivatives or TBBPA mono-ether structural analogs in human samples. Therefore, additional large-scale surveys on the burden to the human body of these chemicals are still needed in the future. The increasing production and usage of TBBPA bis-ether derivates and the continuous transformation into TBBPA mono-ether structural analogs could lead to their higher environmental and human exposure levels (Qu et al. 2013). Currently, the transformation of TBBPA bis-ether derivatives into TBBPA mono-ether structural analogs in the environment has been demonstrated. However, it is unclear whether the TBBPA derivatives could be transformed into TBBPA mono-ether structural analogs by metabolic enzymes in humans, which also needs to be studied in the future. Because some *in vivo* evidence has shown that TBBPA exposure impacted the TH axis, the effect of TBBPA mono-ether structural analogs on the TH system should be given great attention. Comprehensive *in vivo* animal toxicology experiments and human exposure studies are needed in the future and which are important to fully evaluate the risk of these TBBPA structural analogs.

Conclusion

Based on *in vitro* and *in silico* methods with clear mechanisms, we demonstrated the potential TH system–disrupting effects of TBBPA analogs by binding to TTR or TRs. The derivative groups also play a critical role in the cell membrane transportation ability, which in turn determines the effect on GH3 cells. Our study provides clear mechanisms regarding the higher toxicity of TBBPA mono-ether structural analogs than that of TBBPA and TBBPA bis-ether derivatives. To design safer TBBPA derivatives, proper derivative groups should be considered not only for the avoidance of high binding potency to TH receptors but also for the reduction of membrane transportation ability.

Acknowledgments

This work was supported by the National Natural Science Foundation of China (21527901, 21777187, and 21976189), the Sanming Project of Medicine in Shenzhen (No. SZSM201811070), and the Youth Innovation Promotion Association of Chinese Academy of Sciences.

References

Aagaard MM, Siersbæk R, Mandrup S. 2011. Molecular basis for gene-specific transactivation by nuclear receptors. Biochim Biophys Acta 1812(8):824–835, PMID: 21193032, https://doi.org/10.1016/j.bbadis.2010.12.018.

Abou-Elwafa Abdallah M. 2016. Environmental occurrence, analysis and human exposure to the flame retardant tetrabromobisphenol-A (TBBP-A)—a review. Environ Int 94:235–250, PMID: 27266836, https://doi.org/10.1016/j.envint.2016.05.026.

Alaee M, Arias P, Sjödin A, Bergman Å. 2003. An overview of commercially used brominated flame retardants, their applications, their use patterns in different countries/regions and possible modes of release. Environ Int 29(6):683–689, PMID: 12850087, https://doi.org/10.1016/S0160-4120(03)00121-1.

Astapova I, Lee LJ, Morales C, Tauber S, Bilban M, Hollenberg AN. 2008. The nuclear corepressor, NCoR, regulates thyroid hormone action in vivo. Proc Natl Acad Sci USA 105(49):19544–19549, PMID: 19052228, https://doi.org/10.1073/pnas.0804604105.

Bernal J. 2005. Thyroid hormones and brain development. Vitam Horm 71:95–122, PMID: 16112266, https://doi.org/10.1016/S0083-6729(05)71004-9.

Bjoro T, Holmen J, Krüger O, Midthjell K, Hunstad K, Schreiner T, et al. 2000. Prevalence of thyroid disease, thyroid dysfunction and thyroid peroxidase antibodies in a large, unselected population. The Health Study of Nord-Trondelag (HUNT). Eur J Endocrinol 143(5):639–647, PMID: 11078988, https://doi.org/10.1530/eje.0.1430639.

Boas M, Feldt-Rasmussen U, Main KM. 2012. Thyroid effects of endocrine disrupting chemicals. Mol Cell Endocrinol 355(2):240–248, PMID: 21939731, https://doi.org/10.1016/j.mce.2011.09.005.

Bradham KD, Diamond GL, Burgess M, Juhasz A, Klotzbach JM, Maddaloni M, et al. 2018. In vivo and in vitro methods for evaluating soil arsenic bioavailability: relevant to human health risk assessment. J Toxicol Environ Health B Crit Rev 21(2):83–114, PMID: 29553912, https://doi.org/10.1080/10937404.2018.1440902.

Brent GA. 2012. Mechanisms of thyroid hormone action. J Clin Invest 122(9):3035–3043, PMID: 22945636, https://doi.org/10.1172/JCI60047.

Chan WK, Chan KM. 2012. Disruption of the hypothalamic-pituitary-thyroid axis in zebrafish embryo–larvae following waterborne exposure to BDE-47, TBBPA and BPA. Aquat Toxicol 108:106–111, PMID: 22100034, https://doi.org/10.1016/j.aquatox.2011.10.013.

Chen X, Gu J, Wang Y, Gu X, Zhao X, Wang X, et al. 2017. Fate and *o*-methylating detoxification of tetrabromobisphenol A (TBBPA) in two earthworms (*Metaphire guillelmi* and *Eisenia fetida*). Environ Pollut 227:526–533, PMID: 28499262, https://doi.org/10.1016/j.envpol.2017.04.090.

Covaci A, Harrad S, Abdallah MAE, Ali N, Law RJ, Herzke D, et al. 2011. Novel brominated flame retardants: a review of their analysis, environmental fate and behaviour. Environ Int 37(2):532–556, PMID: 21168217, https://doi.org/10.1016/j.envint.2010.11.007.

Covaci A, Voorspoels S, Abdallah MAE, Geens T, Harrad S, Law RJ. 2009. Analytical and environmental aspects of the flame retardant tetrabromobisphenol-A and its derivatives. J Chromatogr A 1216(3):346–363, PMID: 18760795, https://doi.org/10.1016/j.chroma.2008.08.035.

Eng ML, Williams TD, Fernie KJ, Karouna Renier NK, Henry PFP, Letcher RJ, et al. 2019. *In ovo* exposure to brominated flame retardants. Part I: assessment of effects of TBBPA-BDBPE on survival, morphometric and physiological endpoints in zebra finches. Ecotoxicol Environ Saf 179:104–110, PMID: 31026748, https://doi.org/10.1016/j.ecoenv.2019.04.048.

European Commission. 2006. *2,2′,6,6′-Tetrabromo-4,4′-isopropylidene Diphenol (Tetrabromobisphenol-A or TBBPA) Part II—Human Health*. CAS No: 79-94-7, EINECS No: 201-236-9. Summary Risk Assessment Report. https://echa.europa.eu/documents/10162/b1392373-31bd-4722-bf60-fc88225b5a76 [accessed 6 October 2020].

Garmendia Madariaga A, Santos Palacios S, Guillén-Grima F, Galofré JC. 2014. The incidence and prevalence of thyroid dysfunction in Europe: a meta-analysis. J Clin Endocrinol Metab 99(3):923–931, PMID: 24423323, https://doi.org/10.1210/jc.2013-2409.

Gauthier LT, Laurich B, Hebert CE, Drake C, Letcher RJ. 2019. Tetrabromobisphenol-A-bis(dibromopropyl ether) flame retardant in eggs, regurgitates, and feces of herring gulls from multiple North American Great Lakes locations. Environ Sci Technol 53(16):9564–9571, PMID: 31364365, https://doi.org/10.1021/acs.est.9b02472.

Gu J, Jing Y, Ma Y, Sun F, Wang L, Chen J, et al. 2017. Effects of the earthworm *Metaphire guillelmi* on the mineralization, metabolism, and bound-residue formation of tetrabromobisphenol A (TBBPA) in soil. Sci Total Environ 595:528–536, PMID: 28395268, https://doi.org/10.1016/j.scitotenv.2017.03.273.

Gutleb AC, Meerts IATM, Bergsma JH, Schriks M, Murk AJ. 2005. T-screen as a tool to identify thyroid hormone receptor active compounds. Environ Toxicol Pharmacol 19(2):231–238, PMID: 21783481, https://doi.org/10.1016/j.etap.2004.06.003.

Harvey CB, Williams GR. 2002. Mechanism of thyroid hormone action. Thyroid 12(6):441–446, PMID: 12165104, https://doi.org/10.1089/105072502760143791.

Heindel JJ, Blumberg B, Cave M, Machtinger R, Mantovani A, Mendez MA, et al. 2017. Metabolism disrupting chemicals and metabolic disorders. Reprod Toxicol 68:3–33, PMID: 27760374, https://doi.org/10.1016/j.reprotox.2016.10.001.

Hofmann PJ, Schomburg L, Köhrle J. 2009. Interference of endocrine disrupters with thyroid hormone receptor-dependent transactivation. Toxicol Sci 110(1):125–137, PMID: 19403856, https://doi.org/10.1093/toxsci/kfp086.

Huang M, Li J, Xiao Z, Shi Z. 2020. Tetrabromobisphenol A and hexabromocyclododecane isomers in breast milk from the general population in Beijing, China: contamination levels, temporal trends, nursing infant's daily intake, and risk assessment. Chemosphere 244:125524, PMID: 31812044, https://doi.org/10.1016/j.chemosphere.2019.125524.

Jugan ML, Levi Y, Blondeau JP. 2010. Endocrine disruptors and thyroid hormone physiology. Biochem Pharmacol 79(7):939–947, PMID: 19913515, https://doi.org/10.1016/j.bcp.2009.11.006.

Kim UJ, Oh JE. 2014. Tetrabromobisphenol A and hexabromocyclododecane flame retardants in infant–mother paired serum samples, and their relationships with thyroid hormones and environmental factors. Environ Pollut 184:193–200, PMID: 24060738, https://doi.org/10.1016/j.envpol.2013.08.034.

Kitamura S, Jinno N, Ohta S, Kuroki H, Fujimoto N. 2002. Thyroid hormonal activity of the flame retardants tetrabromobisphenol A and tetrachlorobisphenol A. Biochem Biophys Res Commun 293(1):554–559, PMID: 12054637, https://doi.org/10.1016/S0006-291X(02)00262-0.

Kitamura S, Kato T, Iida M, Jinno N, Suzuki T, Ohta S, et al. 2005. Anti-thyroid hormonal activity of tetrabromobisphenol A, a flame retardant, and related compounds: affinity to the mammalian thyroid hormone receptor, and effect on tadpole metamorphosis. Life Sci 76(14):1589–1601, PMID: 15680168, https://doi.org/10.1016/j.lfs.2004.08.030.

Kollitz EM, De Carbonnel L, Stapleton HM, Lee Ferguson P. 2018. The affinity of brominated phenolic compounds for human and zebrafish thyroid receptor β: influence of chemical structure. Toxicol Sci 163(1):226–239, PMID: 29409039, https://doi.org/10.1093/toxsci/kfy028.

Kwon H, Jung JH, Han KD, Park YG, Cho JH, Lee DY, et al. 2018. Prevalence and annual incidence of thyroid disease in Korea from 2006 to 2015: a nationwide population-based cohort study. Endocrinol Metab (Seoul) 33(2):260–267, PMID: 29947180, https://doi.org/10.3803/EnM.2018.33.2.260.

Letcher RJ, Chu S. 2010. High-sensitivity method for determination of tetrabromobisphenol-S and tetrabromobisphenol-A derivative flame retardants in Great Lakes herring gull eggs by liquid chromatography–atmospheric pressure photoionization–tandem mass spectrometry. Environ Sci Technol 44(22):8615–8621, PMID: 20964361, https://doi.org/10.1021/es102135n.

Lévy-Bimbot M, Major G, Courilleau D, Blondeau JP, Lévi Y. 2012. Tetrabromobisphenol-A disrupts thyroid hormone receptor alpha function *in vitro*: use of fluorescence polarization to assay corepressor and coactivator peptide binding. Chemosphere 87(7):782–788, PMID: 22277881, https://doi.org/10.1016/j.chemosphere.2011.12.080.

Liu AF, Qu GB, Yu M, Liu YW, Shi JB, Jiang GB. 2016. Tetrabromobisphenol-A/S and nine novel analogs in biological samples from the Chinese Bohai Sea: implications for trophic transfer. Environ Sci Technol 50(8):4203–4211, PMID: 27008063, https://doi.org/10.1021/acs.est.5b06378.

Liu AF, Qu GB, Zhang CL, Gao Y, Shi JB, Du YG, et al. 2015. Identification of two novel brominated contaminants in water samples by ultra-high performance liquid chromatography-Orbitrap Fusion Tribrid mass spectrometer. J Chromatogr A 1377:92–99, PMID: 25543300, https://doi.org/10.1016/j.chroma.2014.12.038.

Liu AF, Shi JB, Qu GB, Hu LG, Ma QC, Song MY, et al. 2017. Identification of emerging brominated chemicals as the transformation products of tetrabromobisphenol A (TBBPA) derivatives in soil. Environ Sci Technol 51(10):5434–5444, PMID: 28440637, https://doi.org/10.1021/acs.est.7b01071.

Liu AF, Zhao ZS, Qu GB, Shen ZS, Liang XF, Shi JB, et al. 2019. Identification of transformation/degradation products of tetrabromobisphenol A and its derivatives. Trends Analyt Chem 111:85–99, https://doi.org/10.1016/j.trac.2018.12.003.

Liu AF, Zhao ZS, Qu GB, Shen ZS, Shi JB, Jiang GB. 2018. Transformation/degradation of tetrabromobisphenol A and its derivatives: a review of the metabolism and metabolites. Environ Pollut 243(pt B):1141–1153, PMID: 30261454, https://doi.org/10.1016/j.envpol.2018.09.068.

Liu LY, Venier M, Salamova A, Hites RA. 2016. A novel flame retardant in the Great Lakes atmosphere: 3,3′,5,5′-tetrabromobisphenol A bis(2,3-dibromopropyl) ether. Environ Sci Technol Lett 3(5):194–199, https://doi.org/10.1021/acs.estlett.6b00138.

Liu Q, Ren X, Long Y, Hu L, Qu G, Zhou Q, et al. 2016. The potential neurotoxicity of emerging tetrabromobisphenol A derivatives based on rat pheochromocytoma cells. Chemosphere 154:194–203, PMID: 27055180, https://doi.org/10.1016/j.chemosphere.2016.03.117.

Liu QS, Sun Z, Ren X, Ren Z, Liu A, Zhang J, et al. 2020. Chemical structure-related adipogenic effects of tetrabromobisphenol A and its analogues on 3T3-L1 preadipocytes. Environ Sci Technol 54(10):6262–6271, PMID: 32314580, https://doi.org/10.1021/acs.est.0c00624.

Meerts IATM, Assink Y, Cenijn PH, van den Berg JHJ, Weijers BM, Bergman Å, et al. 2002. Placental transfer of a hydroxylated polychlorinated biphenyl and effects on fetal and maternal thyroid hormone homeostasis in the rat. Toxicol Sci 68(2):361–371, PMID: 12151632, https://doi.org/10.1093/toxsci/68.2.361.

Meerts IA, van Zanden JJ, Luijks EAC, van Leeuwen-Bol I, Marsh G, Jakobsson E, et al. 2000. Potent competitive interactions of some brominated flame retardants and related compounds with human transthyretin *in vitro*. Toxicol Sci 56(1):95–104, PMID: 10869457, https://doi.org/10.1093/toxsci/56.1.95.

Mendoza A, Hollenberg AN. 2017. New insights into thyroid hormone action. Pharmacol Ther 173:135–145, PMID: 28174093, https://doi.org/10.1016/j.pharmthera.2017.02.012.

Mengeling BJ, Goodson ML, Furlow JD. 2018. RXR ligands modulate thyroid hormone signaling competence in young *Xenopus laevis* tadpoles. Endocrinology 159(7):2576–2595, PMID: 29762675, https://doi.org/10.1210/en.2018-00172.

Mengeling BJ, Murk AJ, Furlow JD. 2016. Trialkyltin rexinoid-X receptor agonists selectively potentiate thyroid hormone induced programs of *Xenopus laevis* metamorphosis. Endocrinology 157(7):2712–2723, PMID: 27167774, https://doi.org/10.1210/en.2016-1062.

Morte B, Manzano J, Scanlan T, Vennström B, Bernal J. 2002. Deletion of the thyroid hormone receptor α1 prevents the structural alterations of the cerebellum induced by hypothyroidism. Proc Natl Acad Sci USA 99(6):3985–3989, PMID: 11891331, https://doi.org/10.1073/pnas.062413299.

Nyholm JR, Grabic R, Arp HPH, Moskeland T, Andersson PL. 2013. Environmental occurrence of emerging and legacy brominated flame retardants near suspected sources in Norway. Sci Total Environ 443:307–314, PMID: 23201697, https://doi.org/10.1016/j.scitotenv.2012.10.081.

Patrick L. 2009. Thyroid disruption: mechanism and clinical implications in human health. Altern Med Rev 14(4):326–346, PMID: 20030460.

Pullen S, Boecker R, Tiegs G. 2003. The flame retardants tetrabromobisphenol A and tetrabromobisphenol A–bisallylether suppress the induction of interleukin-2 receptor α chain (CD25) in murine splenocytes. Toxicology 184(1):11–22, PMID: 12505372, https://doi.org/10.1016/s0300-483x(02)00442-0.

Qin WP, Li CH, Guo LH, Ren XM, Zhang JQ. 2019. Binding and activity of polybrominated diphenyl ether sulfates to thyroid hormone transport proteins and nuclear receptors. Environ Sci Process Impacts 21(6):950–956, PMID: 31143904, https://doi.org/10.1039/c9em00095j.

Qu G, Liu A, Hu L, Liu S, Shi J, Jiang G. 2016. Recent advances in the analysis of TBBPA/TBBPS, TBBPA/TBBPS derivatives and their transformation products. Trends Analyt Chem 83(pt B):14–24, https://doi.org/10.1016/j.trac.2016.06.021.

Qu GB, Liu AF, Wang T, Zhang CL, Fu JJ, Yu M, et al. 2013. Identification of tetrabromobisphenol A allyl ether and tetrabromobisphenol A 2,3-dibromopropyl ether in the ambient environment near a manufacturing site and in mollusks at a coastal region. Environ Sci Technol 47(9):4760–4767, PMID: 23550727, https://doi.org/10.1021/es3049916.

Qu GB, Shi JB, Wang T, Fu JJ, Li ZN, Wang P, et al. 2011. Identification of tetrabromobisphenol A diallyl ether as an emerging neurotoxicant in environmental samples by bioassay-directed fractionation and HPLC-APCI-MS/MS. Environ Sci Technol 45(11):5009–5016, PMID: 21539307, https://doi.org/10.1021/es2005336.

Ren XM, Guo LH. 2012. Assessment of the binding of hydroxylated polybrominated diphenyl ethers to thyroid hormone transport proteins using a site-specific fluorescence probe. Environ Sci Technol 46(8):4633–4640, PMID: 22482873, https://doi.org/10.1021/es2046074.

Ren XM, Guo LH, Gao Y, Zhang BT, Wan B. 2013. Hydroxylated polybrominated diphenyl ethers exhibit different activities on thyroid hormone receptors depending on their degree of bromination. Toxicol Appl Pharmacol 268(3):256–263, PMID: 23402801, https://doi.org/10.1016/j.taap.2013.01.026.

Roman BR, Morris LG, Davies L. 2017. The thyroid cancer epidemic, 2017 perspective. Curr Opin Endocrinol Diabetes Obes 24(5):332–336, PMID: 28692457, https://doi.org/10.1097/MED.0000000000000359.

Schreiber T, Gassmann K, Götz C, Hübenthal U, Moors M, Krause G, et al. 2010. Polybrominated diphenyl ethers induce developmental neurotoxicity in a human *in vitro* model: evidence for endocrine disruption. Environ Health Perspect 118(4):572–578, PMID: 20368126, https://doi.org/10.1289/ehp.0901435.

Schüttelkopf AW, van Aalten DMF. 2004. PRODRG: a tool for high-throughput crystallography of protein–ligand complexes. Acta Crystallogr D Biol Crystallogr 60(pt 8):1355–1363, PMID: 15272157, https://doi.org/10.1107/S0907444904011679.

Semple KT, Doick KJ, Jones KC, Burauel P, Craven A, Harms H. 2004. Defining bioavailability and bioaccessibility of contaminated soil and sediment is complicated. Environ Sci Technol 38(12):228A–231A, PMID: 15260315, https://doi.org/10.1021/es040548w.

Tang Z, Zhang J, Zhou Q, Xu S, Cai Z, Jiang G. 2020. Thyroid cancer "epidemic": a socio-environmental health problem needs collaborative efforts. Environ Sci Technol 54(7):3725–3727, PMID: 32191442, https://doi.org/10.1021/acs.est.0c00852.

Taylor PN, Albrecht D, Scholz A, Gutierrez-Buey G, Lazarus JH, Dayan CM, et al. 2018. Global epidemiology of hyperthyroidism and hypothyroidism. Nat Rev Endocrinol 14(5):301–316, PMID: 29569622, https://doi.org/10.1038/nrendo.2018.18.

Wang Y, Li Y, Qin Z, Wei W. 2017. Re-evaluation of thyroid hormone signaling antagonism of tetrabromobisphenol A for validating the T3-induced *Xenopus* metamorphosis assay. J Environ Sci (China) 52:325–332, PMID: 28254054, https://doi.org/10.1016/j.jes.2016.09.021.

Yang Y, Ni WW, Yu L, Cai Z, Yu YJ. 2016. Toxic effects of tetrabromobisphenol A on thyroid hormones in SD rats and the derived-reference dose. Biomed Environ Sci 29(4):295–299, PMID: 27241741, https://doi.org/10.3967/bes2016.038.

Yen PM. 2001. Physiological and molecular basis of thyroid hormone action. Physiol Rev 81(3):1097–1142, PMID: 11427693, https://doi.org/10.1152/physrev.2001.81.3.1097.

Yu Y, Ma R, Yu L, Cai Z, Li H, Zuo Y, et al. 2018. Combined effects of cadmium and tetrabromobisphenol A (TBBPA) on development, antioxidant enzymes activity and thyroid hormones in female rats. Chem Biol Interact 289:23–31, PMID: 29702088, https://doi.org/10.1016/j.cbi.2018.04.024.

Yu Y, Xiang M, Gao D, Ye H, Wang Q, Zhang Y, et al. 2016. Absorption and excretion of tetrabromobisphenol A in male Wistar rats following subchronic dermal exposure. Chemosphere 146:189–194, PMID: 26716882, https://doi.org/10.1016/j.chemosphere.2015.12.027.

Zhang YF, Xu W, Lou QQ, Li YY, Zhao YX, Wei WJ, et al. 2014. Tetrabromobisphenol A disrupts vertebrate development via thyroid hormone signaling pathway in a developmental stage-dependent manner. Environ Sci Technol 48(14):8227–8834, PMID: 24963557, https://doi.org/10.1021/es502366g.

Zheng W, Lu YM, Lu GY, Zhao Q, Cheung O, Blaner WS. 2001. Transthyretin, thyroxine, and retinol-binding protein in human cerebrospinal fluid: effect of lead exposure. Toxicol Sci 61(1):107–114, PMID: 11294981, https://doi.org/10.1093/toxsci/61.1.107.

Zhu BR, Zhao G, Yang LH, Zhou BS. 2018. Tetrabromobisphenol A caused neurodevelopmental toxicity via disrupting thyroid hormones in zebrafish larvae. Chemosphere 197:353–361, PMID: 29407805, https://doi.org/10.1016/j.chemosphere.2018.01.080.